Application of CoMFA and CoMSIA 3D-QSAR and Docking Studies in Optimization of Mercaptobenzenesulfonamides as HIV-1 Integrase Inhibitors

Chih-Ling Kuo,[†] Haregewein Assefa,[‡] Shantaram Kamath,[‡] Zdzialaw Brzozowski,[§] Jaroslaw Slawinski,[§] Franciszek Saczewski,[§] John K. Buolamwini,[‡] and Nouri Neamati*,[†]

Department of Pharmaceutical Sciences, School of Pharmacy, University of Southern California, 1985 Zonal Avenue, PSC 304, Los Angeles, California 90089, Department of Pharmaceutical Sciences, College of Pharmacy, University of Tennessee Health Sciences Center, 847 Monroe Avenue Suite 327, Memphis, Tennessee 38163, and Department of Chemical Technology of Drugs, Medical University of Gdansk, 80-416 Gdansk, Poland

An essential step in the HIV life cycle is integration of the viral DNA into the host chromosome. This step is catalyzed by a 32-kDa viral enzyme HIV integrase (IN). HIV-1 IN is an important and validated target, and the drugs that selectively inhibit this enzyme, when used in combination with reverse transcriptase (RT) and protease (PR) inhibitors, are believed to be highly effective in suppressing the viral replication. IN catalyzes two discrete enzymatic processes referred to as 3′ processing and DNA strand transfer. As a part of a study to optimize new lead molecules we previously identified from a series of 2-mercaptobenzenesulfonamides (MBSAs), we applied three-dimensional quantitative structure−activity relationship methods, comparative molecular field analysis (CoMFA), and comparative molecular similarity indices analysis (CoMSIA) to training sets of up to 66 compounds. Two different conformational templates were used: Conf-d, obtained from docking into the HIV-1 IN active site and Conf-s obtained by a systematic conformational search, using lead compounds **1** and **14**, respectively. Reliable models of good predictive power were obtained after removal of compounds with high residuals. The Conf-s models tended to perform better than the Conf-d models. Cross-validated coefficients (q^2) of up to 0.719 (strand transfer CoMSIA, Conf-s) regression coefficients (r^2) of up to 0.932 (strand transfer CoMSIA, Conf-d) were obtained, with the number of partial least squares (PLS) components varying from 3 to 6, and the number of outliers being 4 in most of the models. Because all biological data were determined under exactly the same conditions using the same enzyme preparation, our predictive models are promising for drug optimization. Therefore, these results combined with docking studies were used to guide the rational design of new inhibitors. Further synthesis of 12 new analogues was undertaken, and these were used as a test set for validation of the quantitative structure−activity relationship (QSAR) models. For compounds with closely related structures, binding energies given by the FlexX scoring function correlated with HIV-1 IN inhibitory activity.

Introduction

An obligatory requirement in the retroviral life cycle is the integration of the viral double-stranded DNA into the host chromosome.[1,2] Integrase (IN) catalyzes two separate but chemically similar reactions, known as 3′-processing and strand transfer. In 3′-processing, IN removes a dinucleotide next to a conserved cytosine-adenine sequence from each 3′-end of the viral DNA. IN then attaches the processed 3′-ends of the viral DNA to the host cell DNA in the strand transfer reaction. Because IN has no cellular homologues and is also an essential enzyme for effective viral replication inhibitors of this enzyme are of paramount importance for the treatment of HIV infection.

Many of the identified lead inhibitors of IN were not subsequently optimized to produce a clinically viable candidate (for recent reviews see refs 3 and 4). A lead is defined as a compound that demonstrates a desired biological activity on a validated molecular target. To fulfill the criteria of what the industry considers a useful lead, the compound must exceed a specific potency threshold against the target (e.g., <10 μM inhibition).[5] Many exciting new models for lead discovery have recently emerged that facilitate more rapid identification and result in compounds whose physical and "druglike" properties could be initially optimized. Starting with intuitive structural modification to the development of structure−activity relationship (SAR) and quantitative SAR (QSAR), one can gain tremendous information about the requirement of certain functional groups for activity. To be considered for further development, lead structures should be amenable to chemistry optimization, and have good ADMET (absorption, distribution, metabolism, excretion, and toxicity) properties.[5]

Because the 2-mercaptobenzenesulfonamide (MBSA) class of compounds were potent IN inhibitors and exhibited antiviral activity in cell-based assays with minimal cytotoxicity (see ref 6), we were prompted to

* To whom correspondence should be addressed. (N.N.): Department of Pharmaceutical Sciences, School of Pharmacy, University of Southern California, 1985 Zonal Avenue, PSC 304BA, Los Angeles, CA 90089. Phone: 323−442−2341. Fax: 323−442−1390. E-mail: neamati@usc.edu. Questions regarding modeling studies should be addressed to J.K.B. at jbuolamwini@utmem.edu.
† University of Southern California.
‡ University of Tennessee Health Sciences Center.
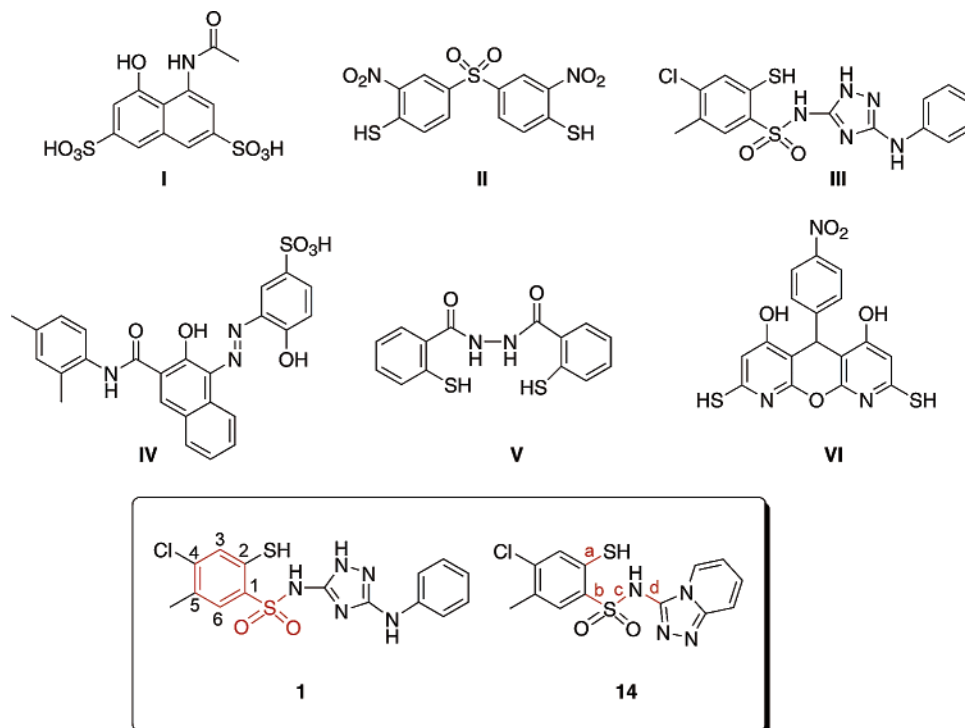§ Medical University of Gdansk.

Figure 1. Structures of mercaptoaryl-containing inhibitors of HIV-1 integase.

employ a detailed QSAR as well as docking studies to better understand their inhibitory properties. Our interest in optimization of the MBSA series of compounds as leads was based on several previous observations. (i) The first 3D-pharmacophore-based study of the NCI database[7] generated a series of sulfonated (e.g., **I**) compounds as inhibitors of IN, and one of those compounds was subsequently cocrystallized with ASV IN, providing the first crystal structure of IN-bound drug.[8] (ii) Among a variety of sulfones (e.g., **II**),[7,9,10] sulfides and sulfonates tested as IN inhibitors, the MBSA class of compounds showed superior antiviral activity in cell-culture (e.g., **III**).[6] (iii) High throughput docking of the NCI database using the cocrystal structure of ASV−IN in complex with compound **I** yielded several sulfonates (e.g., **IV**) and sulfonamides as leads.[10] (iv) Among a series of hydrazides reported by us earlier, the mercaptosalicyl hydrazides (e.g., **V**) were shown to be selective against IN and exhibited antiviral activity.[11] In fact, among the recently reported dipyrimidine inhibitors, only compounds containing a free mercapto group showed antiviral activity and inhibited IN (e.g., **VI**, Figure 1).[12] (v) Availability of numerous analogues tested under the same conditions proved useful in establishing a QSAR model. (vi) In general, these types of structures have shown reduced cytotoxicity and many clinically used antibacterials contain sulfones and sulfonamides (for a recent review see ref 13), making them indeed "druglike".
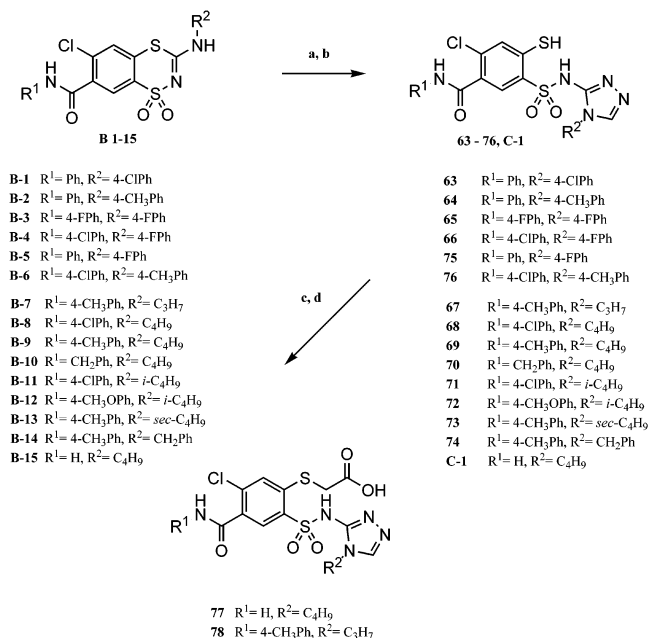
Results and Discussion

Chemistry. The desired 4-chloro-2-mercapto-5-methyl-*N*-(3-arylguanidin-2-yl)benzenesulfonamides **60**−**62** were obtained by reacting *o*-phenylenediamine with corresponding 3-benzoyl-6-chloro-7-methyl-1,1-dioxo-1,4,2-benzodithiazines **A1**−**A3** in toluene under reflux (Scheme 1).

Scheme 1. Synthesis of the 4-Chloro-mercapto-5-methyl-*N*-(3-arylquinoxalin-2-yl)benzenesulfonamides **60**−**62**.
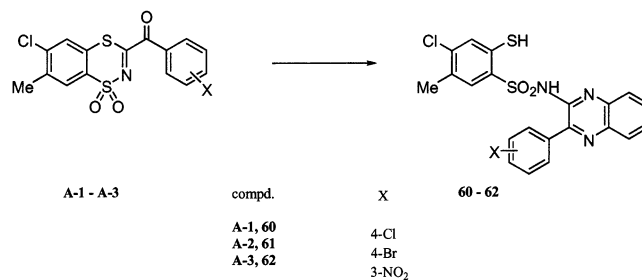
A series of 4-chloro-5-carbamoyl-2-mercapto-*N*-(4*H*-1,2,4-triazol-3-yl)benzenesulfonamides derivatives **63**−**76** and **C-1** were synthesized by the reaction of 3-amino-benzodithiazines (**B-1**−**B-15**)[14−16] with 99% hydrazine hydrate in DMF at 100 °C, as shown in Scheme 2. The reactions were carried out under nitrogen atmosphere to avoid spontaneous air oxidation of the mercaptane functioanlity formed. Then, the 2-mercapto-*N*-(4*H*-1,2,4-triazol-3-yl)benzenesulfonamides **C-1** and **67** were subjected to the reaction with chloroacetic acid under alkaline conditions to give the *S*-alkylated *N*-(4*H*-1,2,4-triazol-3-yl)benzenesulfonamides **77** and **78**, respectively.

Inhibition of HIV-1 IN. The two most extensively studied classes of IN inhibitors are the hydroxylated aromatics and the *β*-diketoacids[17] (for recent reviews see refs 3, 4, and 18). Although the latter class proved to be very promising the hydroxylated aromatics especially of the catechol type have so far not yielded any potential drug candidate. In an effort to develop a new class of IN inhibitors lacking hydroxylated aromatic moieties, which in most cases proved to be responsible for their cytotoxicity and lack of selectivity, we relied on a series of sulfonamides that previously were shown to inhibit

Scheme 2. Synthesis of the 5-Carbamoyl-4-chloro-*N*-(4*H*-1,2,4-triazyn-3-yl)benzenesulfonamides **63**−**78**[a]

B-1 R^1 = Ph, R^2 = 4-ClPh
B-2 R^1 = Ph, R^2 = 4-CH$_3$Ph
B-3 R^1 = 4-FPh, R^2 = 4-FPh
B-4 R^1 = 4-ClPh, R^2 = 4-FPh
B-5 R^1 = Ph, R^2 = 4-FPh
B-6 R^1 = 4-ClPh, R^2 = 4-CH$_3$Ph

B-7 R^1 = 4-CH$_3$Ph, R^2 = C$_3$H$_7$
B-8 R^1 = 4-ClPh, R^2 = C$_4$H$_9$
B-9 R^1 = 4-CH$_3$Ph, R^2 = C$_4$H$_9$
B-10 R^1 = CH$_2$Ph, R^2 = C$_4$H$_9$
B-11 R^1 = 4-ClPh, R^2 = *i*-C$_4$H$_9$
B-12 R^1 = 4-CH$_3$OPh, R^2 = *i*-C$_4$H$_9$
B-13 R^1 = 4-CH$_3$Ph, R^2 = *sec*-C$_4$H$_9$
B-14 R^1 = 4-CH$_3$Ph, R^2 = CH$_2$Ph
B-15 R^1 = H, R^2 = C$_4$H$_9$

63 R^1 = Ph, R^2 = 4-ClPh
64 R^1 = Ph, R^2 = 4-CH$_3$Ph
65 R^1 = 4-FPh, R^2 = 4-FPh
66 R^1 = 4-ClPh, R^2 = 4-FPh
75 R^1 = Ph, R^2 = 4-FPh
76 R^1 = 4-ClPh, R^2 = 4-CH$_3$Ph

67 R^1 = 4-CH$_3$Ph, R^2 = C$_3$H$_7$
68 R^1 = 4-ClPh, R^2 = C$_4$H$_9$
69 R^1 = 4-CH$_3$Ph, R^2 = C$_4$H$_9$
70 R^1 = CH$_2$Ph, R^2 = C$_4$H$_9$
71 R^1 = 4-ClPh, R^2 = *i*-C$_4$H$_9$
72 R^1 = 4-CH$_3$OPh, R^2 = *i*-C$_4$H$_9$
73 R^1 = 4-CH$_3$Ph, R^2 = *sec*-C$_4$H$_9$
74 R^1 = 4-CH$_3$Ph, R^2 = CH$_2$Ph
C-1 R^1 = H, R^2 = C$_4$H$_9$

77 R^1 = H, R^2 = C$_4$H$_9$
78 R^1 = 4-CH$_3$Ph, R^2 = C$_3$H$_7$

[a] Reagents and conditions: (a) H$_2$N-NH$_2$·*x*H$_2$O 99% (6 molar equiv), dry DMF (12 molar equiv), under a nitrogen atmosphere, 100 °C, 15 h (**63**−**66**, **75**, **76**), 10−11 h (**67**−**74**); (b) H$_2$N-NH$_2$·H$_2$O 99% (4 molar equiv), dry DMF (12 molar equiv), under a nitrogen atmosphere, 100 °C, 4 h (**C-1**); (c) NaOH (1 molar equiv), ClCH$_2$CO$_2$H (1 molar equiv), Na$_2$CO$_3$ (1 molar equiv), H$_2$O 40 °C, 1 h, 90−92 °C, 20 h; (d) HCl/H$_2$O.

IN and exhibit antiviral activity in cell culture.[6] We selected three sets of compounds from three separate studies to build a unified model for further drug optimization. The first series of compounds (**1**−**30** and **44**−**47**) were originally discovered as IN inhibitors upon testing approximately 5000 compounds that were selected by the National Cancer Institute (NCI) Drug Synthesis and Chemistry Branch as compounds with antiviral activity in cell-based assays.[6] The second series of compounds (**31**−**43** and **48**) were discovered using a three-point pharmacophore searching of the NCI database.[7] The third series of compounds (**49**−**54**) were selected from a high throughput docking of the NCI database using the X-ray structure of ASV integrase in complex with a naphthalene bisulfonate, Y3.[10] Moreover, a series of new compounds (**55**−**66**) that was initially synthesized to answer the question of the nature of the free mercapto group and substitution on the sulfonamide moiety were also included in our training set for our QSAR models (see below). Compounds **55**−**66** showed very promising activity against purified IN.

In the previous report, the data indicated that the bulkier group (two-rings and three-rings) substituted on the N of the sulfonamide moiety was responsible for enhanced potency. As expected, compounds **60**−**66** all inhibited IN at low micromolar levels. Moreover, we earlier showed that some compounds with an acetate group at R$_5$-position were more potent than compounds having a methyl substituent at this position.[6] Thus, compound **63**−**66** were synthesized and tested for their ability to inhibit IN. Compound **63** and **64** showed IC$_{50}$ values of 6 and 12 *μ*M for 3′-processing and strand

transfer inhibition, respectively, while the IC$_{50}$ values of compounds **65** and **66** were 80 and 37 *μ*M, respectively.

In using the 3D-QSAR and docking analyses reported here to optimize these sets of molecules and to further investigate how the substituents on the triazolo ring and amide affect the activity of compounds, compounds **67**−**78** were designed and synthesized. The QSAR models tended to attribute high inhibitory activities to these compounds, and the docking studies predicted them to be among the high affinity ligands. Among these new analogues, compound **76** with IC$_{50}$ values of 4 *μ*M against both 3′-processing and strand transfer activities was the most potent. Interestingly, the FlexX docking study predicted it to have the highest binding affinity among the test set compounds. A subtle shift in potency was observed when comparing compounds with different substitution at the R$_1$ group. Interestingly, when the IC$_{50}$ value of compound **76** was compared with those of the corresponding alkyl analogues (**68** and **71**), the presence of the phenyl ring increased the activity by 10-fold. The docking also suggested that the compounds with the phenyl ring generally bound the enzyme with higher affinity (see FlexX scores). Surprisingly, the activities of the compounds (**77** and **78**), in which the mercapto group was protected, were not abolished. Compound **78** still retains the activity of compound **67**. Compound **77** has an IC$_{50}$ value of 333 *μ*M, although it is 5 times higher than that of compound **69**. This may be due to the possibility that under the experimental condition the carboxylic group will be ionized. On the basis of these data, several pertinent features emerge to be important for IN inhibition. Substituting a bulky group at 5-position and at sulfonamide may enhance potency. Furthermore, a negative charge at 2-position is important for activity and the mercapto group at 2-position is important for high activity, but may not be essential.

3D-QSAR Modeling. Partial least squares (PLS), the statistical method used in deriving the 3D QSAR models, is an extension of multiple regression analysis in which the original variables are replaced by a small set of their linear combinations.[19−21] These latent variables (components) so generated are used for multivariate regression, maximizing the commonality of explanatory and response variable blocks. PLS has been useful in cases in which the number of descriptors is greater than the number of samples (compounds) as is the case with comparative molecular field analysis (CoMFA) and comparative molecular similarity indices analysis (CoMSIA) 3D QSAR analyses.

Leave-one-out (LOO) cross-validated PLS analyses were used to check the predictive ability of the models and to determine the optimal number of components to be used in the final QSAR models. The training sets with the 3′-processing and strand transfer inhibitory activities were composed of **66** and **64** compounds, respectively. To generate a reasonable model in most cases, four compounds were removed as outliers. In one case, only two outliers were eliminated, whereas in another case six compounds were eliminated from the training set. Compounds **36** and **48** were common outliers in CoMFA and CoMSIA models based on 3′-processing inhibitory activity data, while compounds **36**

and **57** were common outliers in models based on strand transfer inhibitory activities. Compound **36** tended to be an outlier in all QSAR models. This compound is the only molecule with an aliphatic carboxylic acid substituent at the 4-position. Compound **48**, which was a common outlier in the 3′-processing models, is also structurally different in terms of the substituents at the 4-position and on the sulfonamide group. Structural uniqueness underscores the outlier status of compounds for the most part.

Results of the PLS analyses are summarized in Table 3. Group cross-validation (10 groups) and scrambling of the biological data (randomization control) were performed to test the stability and reliability of the models. The average q^2 values obtained in the group cross-validation and randomization exercises are presented in Table 4. These results indicate stability in the CoMFA and CoMSIA QSAR models. The predictive ability of the models was further validated using the external test set of 12 compounds (see Table 2) in both Conf-d and Conf-s conformations. The prediction of activities for training set and test set compounds by the different QSAR models generated are presented in graphical form in Figures 2 and 3. The predictions for the training set are shown as filled circles, whereas open circles indicate predictions for the test set. In Figures 2 and 3, the solid line represents the regression fitted line of the training set whereas the dotted line shows the error limit of ± 1 log unit about the corresponding fitted curve. The residuals from the prediction of the test set by the final QSAR models are shown in Table 5.

CoMFA Using the Inhibition of 3′-Processing Reaction. With the 3′-processing inhibitory activity as a response variable, initial CoMFA PLS analyses of the 66 compounds gave low q^2 values. Removal of outliers based on residual values afforded models with q^2 values of 0.557 and 0.630 for Conf-d and Conf-s models, respectively (Table 3). For the two conformational sets, r^2 values of 0.921 and 0.858 were obtained for Conf-d and Conf-s models, respectively. The graph of the actual pIC_{50} versus the predicted pIC_{50} values for the training set and test set compounds by the CoMFA models based on 3′-processing are shown in Figure 2a,b. CoMFA predictions with both Conf-d and Conf-s show a similar trend. However, the Conf-s models performed better. Examination of the residuals from the prediction (Table 5) shows that the inhibitory activities of 10 of the 12 compounds were predicted within ± 1 unit of the actual pIC_{50} values by the model based on Conf-d, whereas the Conf-s models predicted all 12 compounds well within the ± 1 unit. In this instance, the model with a better q^2, and in which fewer outliers had to be removed (Conf-s model) afforded a better predictive model. The Conf-s model predicted the test set better than the Conf-s possibly because the Conf-s had more structural representatives than the Conf-d as far as the test set is concerned.

The CoMFA PLS stdev*coefficient contour maps for the 3′-processing inhibitory activity, are shown in Figure 4A,B. In both figures, a yellow contour near the 4-position of the common aromatic ring indicates that bulky substituents at this position decrease activity. This is reflected in compounds **31**, **35**, **37**, and **39−42**, which have bulky substituents at this position and have pIC_{50}

values below 4.0. Compounds **49−54**, which have pIC_{50} values above 4.0, are exceptions. This might be due to the H-bond donor groups on the substituent moieties, the interactions of which probably offset the steric effects. Both the green contours appearing near the 5-position of the aromatic ring in Figure 4A and the green contour map in Figure 4B stretching toward the 5-position of the aromatic ring suggest that a bulky substituent at this position will enhance inhibitory potency. A comparison of compounds **2** and **44** shows that a change from a methyl to an acetate group at the 5-position increases the potency, which may be due to an increase in the steric bulk of the group. The relatively lower potency of compounds **45** and **46** as compared to compounds **17** and **18** may be due partly to the absence of any substituent at position 5. Compounds **63** and **64**, which have an N-phenyl carbamoyl substituent, have high potencies possibly due to the relatively larger substituent at this position. However, further increase in the size of the substituent appears to decrease the potency as shown by compounds **65** and **66**. A green contour around the phenylamino group attached to the triazole ring in both Figure 4A,B suggests that bulky substituents at this location might enhance potency. Compounds with bulky substituents at this site such as **3−5**, **8−9**, **12**, **13**, **17−23**, and **25−28** have retained high potency. The yellow contour on the other side of the triazole ring shows that a bulky substituent around that region would decrease potency. Red contours surrounding the triazole ring show that high electron density (electronegative groups) favors inhibitory activity. The relatively low potency of compounds **55−59**, which have a positive charge around this area, shows the preference of a negative charge over a positive charge.

CoMFA Using the Inhibition of Strand Transfer Reaction. Using the strand transfer inhibitory activity as a response variable, CoMFA PLS analyses of all the 64 compounds resulted in q^2 values of 0.596 and 0.679 for the Conf-d and Conf-s conformational sets, respectively, with removal of four outlier compounds. The r^2 values for the final CoMFA models are 0.797 and 0.892 for the Conf-d and Conf-s conformational sets, respectively (see Table 3). The plots of the predicted against actual pIC_{50} values for the training and test sets are shown in Figure 3a.

The residuals from the prediction of the test set compounds by the Conf-d and Conf-s CoMFA models are shown in Table 5. The Conf-d models predicted 11 of the 12 test compounds within ± 1 unit of the actual pIC_{50} values, whereas the Conf-s was able to predict all 12 test compounds within ± 1 pIC_{50} unit. Comparing the two conformational sets, the Conf-s again performed better in predicting the activity of the test set. This superiority is also reflected in the q^2 and r^2 values. The CoMFA PLS contour maps for strand transfer inhibitory activity (data not shown) suggest structure−activity relationships similar to those of 3′-processing CoMFA contour maps.

CoMSIA Studies Using the Inhibition of 3′-Processing Reaction. CoMSIA PLS analysis of the 66 compounds using the 3′-processing inhibitory activity as a response variable afforded models with q^2 values of 0.594 (Conf-d) and 0. 0.658 (Conf-s), and r^2 values of

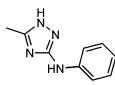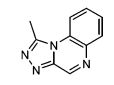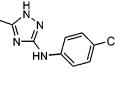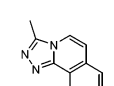**Table 1.** Structures, Activities, and Docking Energies of Compounds in the Training Set
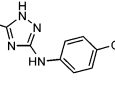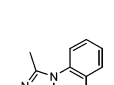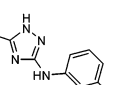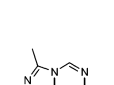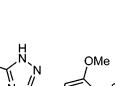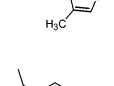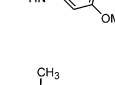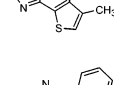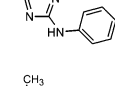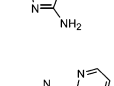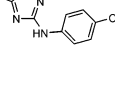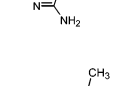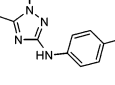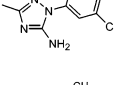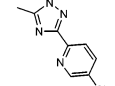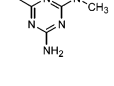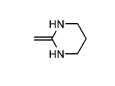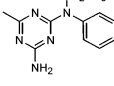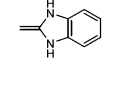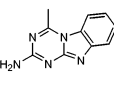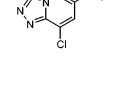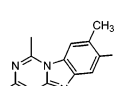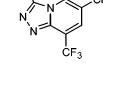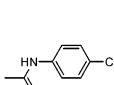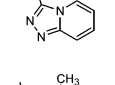
Compd.	R	pIC$_{50}$		FlexX score	Compd.	R	pIC$_{50}$		FlexX score
		3'-Proc.	Strand transfer	kcal/mole			3'-Proc.	Strand transfer	kcal/mole
1		4.79	4.90	-18.6	**16**		4.50	5.08	-15.1
2		4.65	4.62	-18.6	**17**		4.88	4.97	-14.6
3		4.81	4.85	-18.3	**18**		4.89	5.13	-15.1
4		5.20	4.68	-19.8	**19**		5.44	5.46	-15.3
5		4.81	4.78	-19.3	**20**		5.03	5.13	-14.8
6		4.56	4.80	-18.3	**21**		4.97	4.88	-18.6
7		4.63	4.72	-18.0	**22**		4.84	4.64	-18.5
8		4.79	4.75	-18.0	**23**		5.03	5.20	-17.4
9		5.05	4.99	-15.0	**24**		4.11	4.38	-14.9
10		3.83	3.84	-12.1	**25**		4.76	4.61	-14.9
11		4.41	4.36	-13.7	**26**		5.01	5.11	-16.2
12		4.75	4.68	-13.5	**27**		5.26	5.37	-13.3
13		4.97	4.62	-13.0	**28**		5.45	5.45	-21.1
14		3.91	3.96	-16.1	**29**		4.06	4.00	-20.5
15		4.73	4.96	-12.1					

Table 1 (Continued)
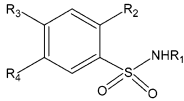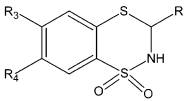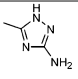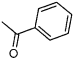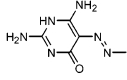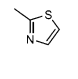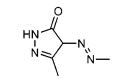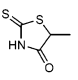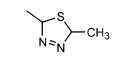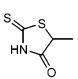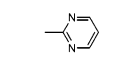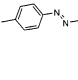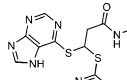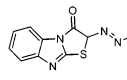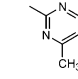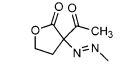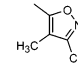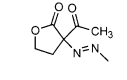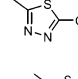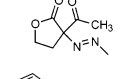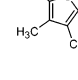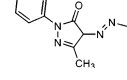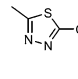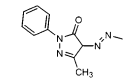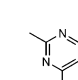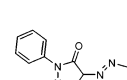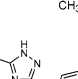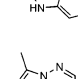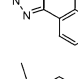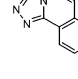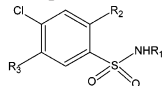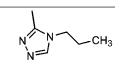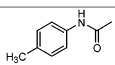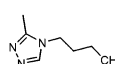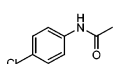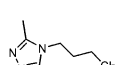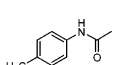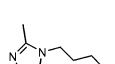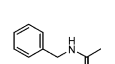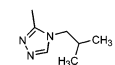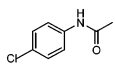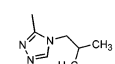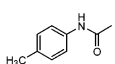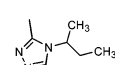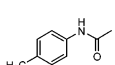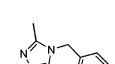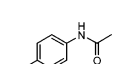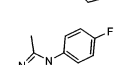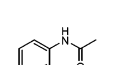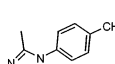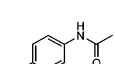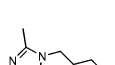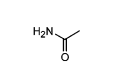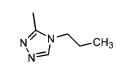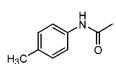
Compd.	Struct.	R_1	R_2	R_3	R_4	pIC$_{50}$ 3'-Proc	ST	FlexX score kcal/mole
30	A	(structure)	$SCH_2CO_2^-$ CH_3	Cl	CH_3	3.70	-	-14.9
31	A	(structure)	H	(structure)	H	3.92	4.02	-24.3
32	A	(structure)	H	(structure)	H	4.15	4.21	-18.1
33	A	(structure)	H	(structure)	H	4.62	4.72	-18.4
34	A	(structure)	H	(structure)	H	4.54	4.85	-15.4
35	A	(structure)	H	(structure)	H	3.85	3.95	-20.2
36	A	NH_2	H	OCH_2COOH	H	5.09	5.06	-17.3
37	A	H	H	(structure)	H	3.68	3.90	-17.2
38	A	(structure)	H	(structure)	H	4.15	4.19	-16.8
39	A	(structure)	H	(structure)	H	3.71	3.84	-21.7
40	A	(structure)	H	(structure)	H	3.61	3.75	-20.8
41	A	(structure)	H	(structure)	H	3.89	3.97	-20.3
42	A	(structure)	H	(structure)	H	3.87	4.11	-21.5
43	A	(structure)	H	(structure)	H	4.31	4.63	-21.2
44	A	(structure)	SH	Cl	$OCOCH_3$	5.12	5.00	-22.9
45	A	(structure)	SH	Cl	H	4.54	4.41	-15.9
46	A	(structure)	SH	F	H	4.29	4.32	-12.6
47	A	(structure)	SH	Cl	H	4.66	4.71	-11.6

Table 1 (Continued)

A   B

Compd.	Struct.	R_1	R_2	R_3	R_4	pIC$_{50}$		FlexX score kcal/mole
						3'-Proc	ST	
48	A	(CH$_2$CH$_2$OH)$_2$	H		H	5.30	-	-14.5
49	A		H		H	4.67	4.37	-20.9
50	A		H		H	4.41	4.30	-20.3
51	A		H		H	4.71	4.49	-18.9
52	A		H		H	4.22	4.23	-21.5
53	A		H		H	4.18	4.14	-18.4
54	A		H		H	4.64	4.68	-20.5
55[a]	B		-	Cl	CH$_3$	4.22	4.22	-21.5
56[a]	B		-	Cl	CH$_3$	4.22	4.30	-18.7
57[a]	B		-	Cl	CH$_3$	3.15	3.22	-16.5
58[a]	B		-	Cl	CH$_3$	3.70	3.95	-17.4
59[a]	B		-	Cl	CH$_3$	3.48	3.95	-13.2
60	A		SH	Cl	CH$_3$	4.70	4.92	-17.6
61	A		SH	Cl	CH$_3$	4.91	5.10	-17.3
62	A		SH	Cl	CH$_3$	4.82	5.10	-21.4
63	A		SH	Cl		5.22	4.92	-25.0
64	A		SH	Cl		5.22	5.00	-25.2
65	A		SH	Cl		4.10	4.43	-25.0
66	A		SH	Cl		4.43	4.43	-25.4

[a] These compounds are diaminopyridine salts. ST: Strand Transfer.

Table 2. Structures, Activities, and Docking Energies of Compounds in the Training Set[a]

Compd	R₁	R₂	R₃	pIC₅₀		FlexX score
				3'-Proc	ST	kcal/mole
67		SH		4.39	4.40	-21.9
68		SH		4.44	4.36	-20.4
69		SH		4.22	4.47	-20.7
70		SH		4.05	4.15	-18.9
71		SH		4.42	4.40	-21.5
72		SH		4.12	4.00	-21.9
73		SH		3.70	3.95	-19.2
74		SH		5.05	5.10	-21.7
75		SH		4.34	4.30	-24.3
76		SH		5.40	5.40	-24.9
77		SCH₂COOH		3.38	3.38	-21.8
78		SCH₂COOH		4.36	4.36	-23.6

[a] ST: strand transfer.

0.917 and 0.909 for Conf-d and Conf-s sets, respectively. Only two and three compounds were removed as outliers in the respective conformational sets. Figure 2c,d depicts the fitted prediction curves of the training set and predictions of the test set by the Conf-d and Conf-s CoMSIA models, respectively. The differences in q^2 values of the models are reflected in their ability to predict the activities of the test set compounds (Table 5). As shown in Table 5, the CoMSIA model of the Conf-d set predicted nine of the 12 test compounds within ±1 pIC₅₀ units of the actual pIC₅₀ values, whereas the CoMSIA model of the Conf-s set predicted 11 of the compounds with a similar precision. The Conf-d CoMSIA model for 3′-processing is better than the corresponding CoMFA model, but that is not the case with the Conf-s models in which the CoMFA model outperforms the corresponding CoMSIA model.

The CoMSIA hydrophobic and H-bonding descriptors PLS contour maps for the Conf-d and Conf-s conformational sets are shown in Figure 4, panels C and D, respectively. The cyan contours near the sulfonamide

NH in Figure 4C,D show that a H-bond donor group in this area enhances potency. There is a H-bond acceptor magenta contour around the sulfonyl oxygens and mercapto sulfur consistent with the docking. The other salient feature about the CoMSIA contour maps is the indication of a significant hydrophobic contribution (white contour) at the R₁ substituent and the edge of the common substituted phenyl ring around the chlorine substituent. This reflects the significant contribution of the hydrophobic descriptor to the CoMSIA QSAR models, which is the single most important contributor (see Table 3). The preponderance of the steric fields in the CoMFA models may also reflect this hydrophobic contribution, which may be implicit in steric bulk allowed regions.

CoMSIA Using the Inhibition of Strand Transfer Reaction. PLS analysis of the CoMSIA descriptors using the strand transfer inhibitory activity gave q^2 values of 0.637 and 0.719 for the Conf-d and for the Conf-s sets, respectively. The r^2 values are 0.923 for the Conf-d and 0.913 for Conf-s. The residuals in Table 5

Figure 2. CoMFA and CoMSIA predictions for the training (●) and test (○) sets for 3′ processing. The fitted curves for CoMFA models using Conf-d and Conf-s sets are shown in panels a and b, respectively, whereas the corresponding curves for the CoMSIA models are shown in panels c and d, respectively. The solid line is the regression line for the training set predictions, whereas the dotted lines indicate the ± 1.0 log point error margins.

Table 3. CoMFA and CoMSIA PLS Statistics

PLS statistics	CoMFA				CoMSIA			
	3′ processing		strand transfer		3′ processing		strand transfer	
	Conf _d	Conf_s	Conf_d	Conf _s	Conf_d	Conf_s	Conf_d	Conf_s
q^2	0.557	0.630	0.596	0.679	0.594	0.658	0.637	0.719
PRESS	0.372	0.331	0.291	0.257	0.348	0.318	0.282	0.240
r^2	0.921	0.858	0.790	0.892	0.917	0.909	0.923	0.913
s	0.157	0.205	0.210	0.149	0.158	0.164	0.131	0.134
F	102.61	67.66	68.77	72.69	104.74	92.97	107.69	93.104
no. of outliers	6	4	4	4	2	3	2	4
PLS comp	6	5	3	6	6	6	6	6
contribution:								
steric	0.658	0.569	0.610	0.582	0.158	0.162	0.175	0.148
electrostatic	0.342	0.431	0.390	0.418	0.204	0.307	0.215	0.133
hydrophobic					0.260	0.266	0.239	0.265
H-bond donor					0.145	0.266	0.160	0.207
H-bond acceptor					0.199	0.175	0.211	0.247

Table 4. Group Validation and Randomization Exercises

set	exercise	average PLS statistics	3′-processing		strand transfer	
			CoMFA	CoMSIA	CoMFA	CoMSIA
Conf_d	group validation	q^2 (std)	0.557 (0.030)	0.569 (0.033)	0.595 (0.018)	0.628 (0.021)
	randomization	q^2	−0.179	−0.276	−0.156	−0.145
Conf_s	group validation	q^2 (std)	0.625 (0.016)	0.639 (0.028)	0.671 (0.033)	0.688 (0.031)
	randomization	q^2	−0.223	−0.216	−0.173	−0.173

show that the Conf-d set performed a little better at predicting the activities of the external test set in which 11 of the 12 compounds were predicted within ±1 pIC$_{50}$ unit of the actual activity. The Conf-s CoMSIA model predicted 10 compounds within the same boundaries (Figure 3d). The CoMSIA contour maps for both the Conf-s and Conf-d (data not shown) were similar to the

CoMSIA contour maps of the models generated using 3′-processing inhibitory activity as a dependent variable.

Docking Studies. All the molecules in a database containing both the training and test sets were docked onto the monomeric unit A of the crystal structure of HIV-1 IN catalytic core (PDB 1QS4). Among the 30 possible docking structures of compound **1** generated by

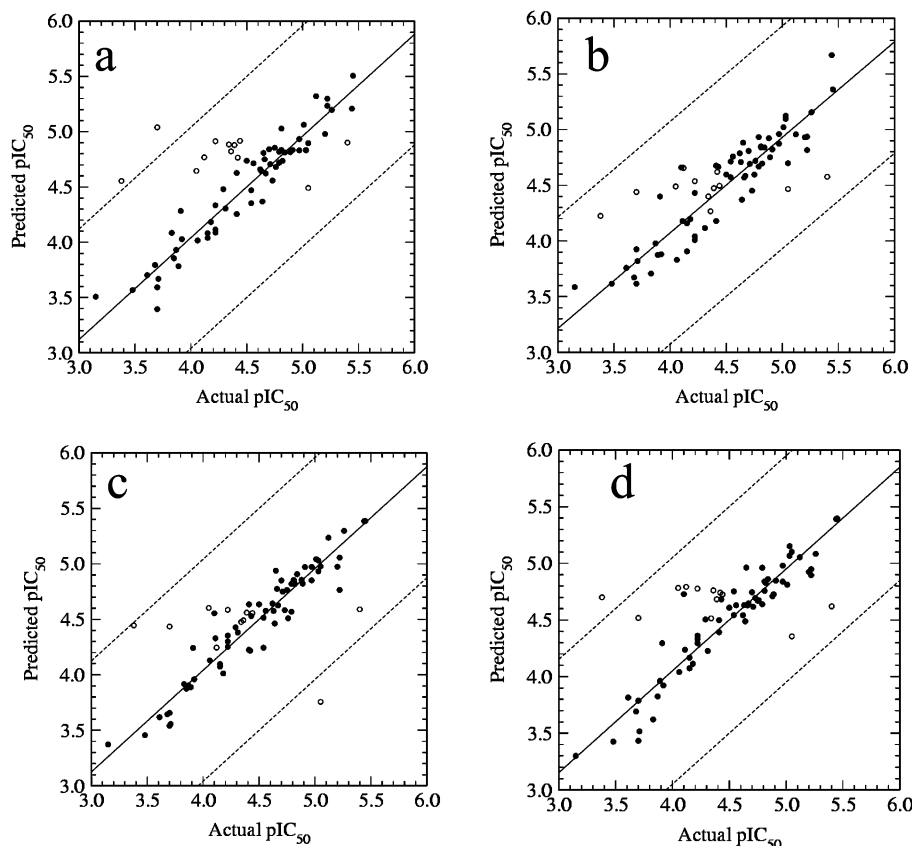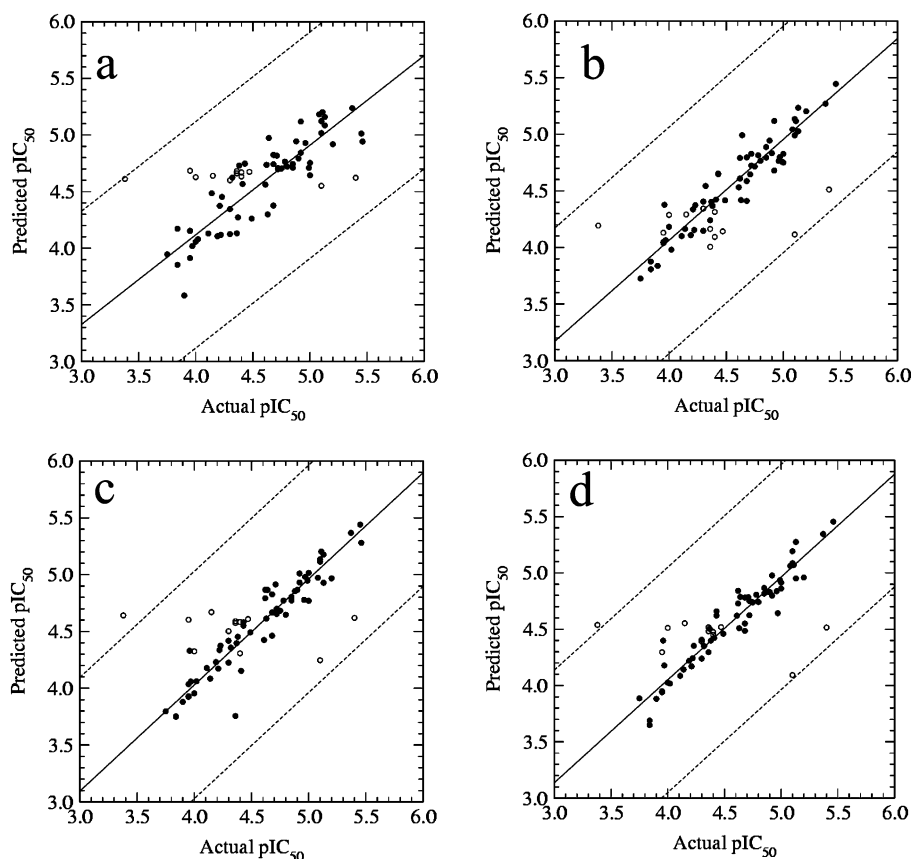**Figure 3.** CoMFA and CoMSIA predictions for the training (●) and test (○) sets for strand transfer activity. The fitted curves for CoMFA models using Conf-d and Conf-s sets are shown in panels a and b, respectively, whereas the corresponding curves for the CoMSIA models are shown in panels c and d, respectively. The solid line is the regression line for the training set predictions whereas the dotted lines indicate the ± 1.0 log point error margins.

Table 5. Residuals of the Prediction of the Test Set by CoMFA and CoMSIA Models

		residuals					residuals			
		CoMFA		CoMSIA			CoMFA		CoMSIA	
compd	3'-Proc. pIC_{50}	Conf_d	Conf_s	Conf_d	Conf_s	strand transfer pIC_{50}	Conf_d	Conf_s	Conf_d	Conf_s
67	4.39	−0.489	−0.084	−0.170	−0.293	4.40	−0.271	0.307	−0.183	−0.050
68	4.44	−0.477	−0.055	−0.116	−0.285	4.36	−0.321	0.197	−0.230	−0.122
69	4.22	−0.694	−0.316	−0.365	−0.557	4.47	−0.204	0.328	−0.139	−0.049
70	4.05	−0.595	−0.439	−0.553	−0.733	4.15	−0.489	−0.141	−0.520	−0.403
71	4.42	−0.345	−0.200	0.203	−0.321	4.40	−0.233	0.089	0.093	−0.076
72	4.12	−0.648	−0.535	−0.125	−0.672	4.00	−0.627	−0.287	−0.325	−0.512
73	3.70	−1.339	−0.739	−0.735	−0.818	3.95	−0.734	−0.180	−0.653	−0.346
74	5.05	0.559	0.584	1.294	0.695	5.10	0.549	0.986	0.854	1.007
75	4.34	−0.544	−0.060	−0.136	−0.174	4.30	−0.300	−0.043	−0.202	−0.091
76	5.40	0.499	0.824	0.810	0.780	5.40	0.778	0.889	0.781	0.885
77	3.38	−1.174	−0.845	−1.065	−1.32	3.38	−1.232	−0.813	−1.261	−1.158
78	4.36	−0.462	0.094	−0.131	−0.401	4.36	−0.301	0.355	−0.214	−0.158

the FlexX docking program, the conformation that was indicated as the most tightly bound by FlexX scoring, overlapped with the cocrystallized inhibitor. Figure 5a shows the cocrystallized compound in magenta and the highest ranked conformation of compound **1** in ball-and-stick rendering. This conformation of compound **1** was used to build the rest of the molecules in the Conf-d set. Figure 5b shows the CoMFA steric contour plot of the Conf-d set for the 3'-processing inhibitory activity projected onto the Connolly surface of the active site of HIV-1 IN. As shown in this figure, the steric plot agrees well with the topology of the IN active site, showing yellow contours in regions of the active site with restriction against bulky substituents and green contours in regions of the active site that will accommodate further substitution on the molecule.

The FlexX docking energy of the compounds in the training set did not show a general correlation with their 3'-processing or strand transfer inhibitory activities (Tables 1 and 2). Examination of the FlexX docked structures of the compounds in the training set also showed that most of the molecules did not have a common binding mode. The wide range of binding modes adopted by the molecules, as well as the lack of general correlation between the docking energy and inhibitory activities, may be due to the large structural differences existing among the compounds.

On the other hand, most of the compounds in the test set bound in a similar mode due to their close structural similarity. Compounds **63**−**66** from the training set, which are structurally similar to the compounds in the test set, also adopted a binding mode similar to that of
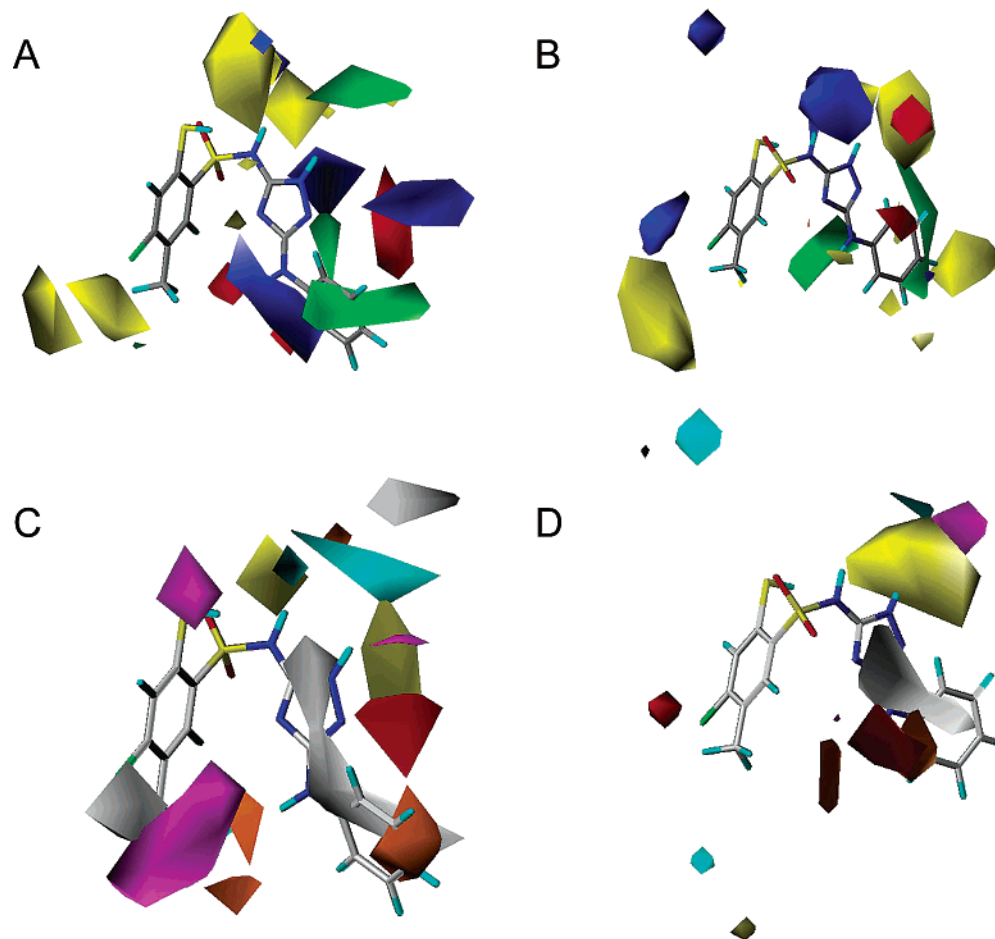
Figure 4. Contour maps of CoMFA and CoMSIA 3D-quantitative structure-3′-end processing activity relationships. (A) Conf-d CoMFA contour map; green contours indicate regions where a bulky substituent increases potency, yellow shows areas where bulky substituents decreases potency. (B) Conf-s CoMFA contour maps; color designation are same as the Conf-s contour map. (C) Conf-d CoMSIA hydrophobic, hydrogen bond donor, and hydrogen bond acceptor contour maps; white shows areas where hydrophobic groups enhance potency, whereas yellow indicates that such groups decrease potency. Cyan indicates areas where hydrogen bond donor groups increase potency, whereas orange indicates the opposite. Areas where a hydrogen bond acceptor moiety favors activity are indicated by magenta, while areas where a hydrogen bond acceptor group decreases activity are shown by red. (D) Conf-s CoMSIA hydrophobic, hydrogen bond donor, and hydrogen bond acceptor contour maps; color designations are the same as in panel C.

the test set compounds. Interestingly, the FlexX energy scores of these compounds from the training set and those of the test set compounds correlated well with their 3′-processing and strand transfer inhibitory activities (Figure 6). This is noteworthy since the general experience has been that the available docking scoring functions perform poorly in predicting experimental binding affinities. It indicates that FlexX docking may be useful in optimizing these compounds.

Experimental Section

Chemistry. The following substrates: 3-aroyl-1,1-dioxo-1,4,2-benzodithiazines **A-1**−**A-3**[22] and 3-amino-7-carbamoyl-6-chloro-1,1-dioxo-1,4,2-benzodithiazines **B-1**−**B-6**[23] and **B-7**−**B-15**.[23,24] as well as final products: **30**,[25] **44**,[26] **45**,[27] **46**,[27] **47**[27] and **55**−**59**[28] were obtained according to the described procedures.

Melting points were determined using a Buchi SMP 20 apparatus and are uncorrected. IR spectra in KBr were recorded on a Perkin-Elmer 1600 FTIR spectrophotometer. ^{1}H and ^{13}C NMR spectra were recorded on a Varian Gemini 200 at 200 and 50 MHz, respectively; chemical shifts are reported in parts per million (ppm) relative to TMS. The following abbreviations are used to describe peaks patterns when appropriate: b = broad, s = singlet, d = doublet, t = triplet,

q = quartet, m = multiplet. The results of elemental analyses for C, H, and N were within ±0.4% of the theoretical values.

General Procedure for the Preparation of 4-Chloro-2-mercapto-5-methyl-*N*-(3-arylquinoxalin-2-yl)benzene-sulfonamides 60−**62.** A stirred solution of *O*-phenylenediamine (0.45 g, 0.0042mol) and the appropriate arolylbenzodithiazine **A-1**, **A-2**, or **A-3** (0.004 mol) in anhydrous toluene (35 mL) was refluxed for 9 h. Then, toluene (15 mL) was evaporated under reduced pressure and the solid that precipitated upon cooling to room temperature was filtered off and washed with toluene (3 × 2 mL).

In this manner the following sulfonamides were obtained:

4-Chloro-[3-(4-chlorophenyl)quinoxalin-2-yl]-2-mercapto-5-methylbenzene-sulfonamide (60). Starting from 6-chloro-3-(4-chlorobenzoyl)-7-methyl-1,1-dioxo-1,4,2-benzodithiazine (1.55 g) the compound **60** was obtained (1.6 g, 84%): mp 183−185 °C dec; IR (KBr) 3235, 3165 (NH), 2520 (SH), 1615 (C=N), 1345, 1150 (SO$_2$) cm^{-1}; ^{1}H NMR (CDCl$_3$) δ 2.37 (s, 3H, CH$_3$), 4.64 (br. s, 1H, SH), 7.39−7.69 (m, 6H, arom), 7.94−8.06 (m, 4H, arom), 12.18 (br.s, 1H, NH) ppm; ^{13}C NMR (CDCl$_3$) δ 20.00, 117.20, 125.65, 127.09, 128.79, 130, 36, 131.41, 131.49, 131.66, 131.92, 132.14, 133.96, 134.22, 137.27, 139.35, 141.40 ppm. Anal. (C$_{21}$H$_{15}$Cl$_2$N$_3$O$_2$S$_2$) C, H, N.

***N*-[3-(4-Bromophenyl)quinoxalin-2-yl]-4-chloro-2-mercapto-5-methylbenzene-sulfonamide (61).** Starting from 3-(bromobenzoyl)-6-chloro-7-methyl-1,1-dioxo-1,4,2-benzodithi-
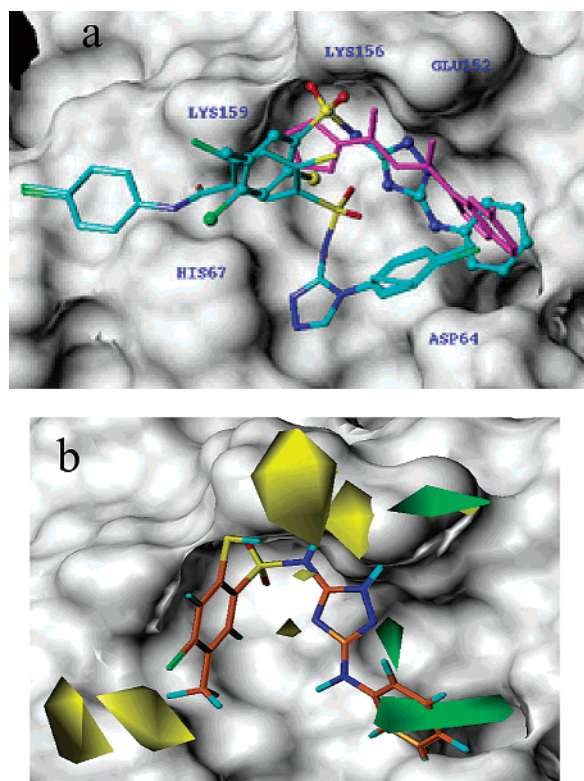
Figure 5. FlexX docked structures. (a) Representative docked structures of the training and test sets: compound colored magenta is the cocrystallized HIV-1 integrase inhibitor in the active site; compound in ball-and-stick rendering is the FlexX docked structure of compound **1**, carbon atoms are colored cyan, nitrogen atoms blue, sulfur atoms yellow, and oxygen atoms red; capped stick structures are compounds in the training set, and most of the test set compounds that showed common binding mode from FlexX docking. (b) Conf-d CoMFA steric contour map projected onto Connolly surface of HIV-1 integrase active site.

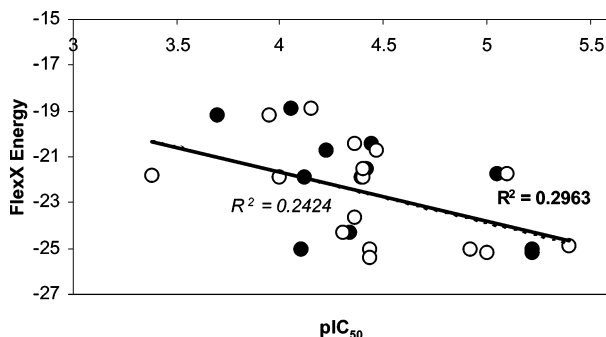**Figure 6.** Plots of pIC_{50} vs FlexX docking energy (kcal/mol) for compounds from the training and the test sets with close structural similarity; filled circles, solid lines and nonitalicized coefficient of determination (R^2) represent 3′-end processing data, while open circles, dotted lines, and italicized coefficient of determination (R^2) represent strand transfer data.

azine (1.73 g), the compound **61** was obtained (1.8 g, 89%): mp 172−174 °C dec; IR (KBr) 3230, 3170 (NH), 2545 (SH), 1610 (C=N), 1345, 1130 (SO₂) cm⁻¹; ¹H NMR (CDCl₃) 2.34 (s, 1H, SH), 2.37 (s, 3H, CH₃), 7.39 (s, 1H, H-3, PhSO₂), 7.42−7.65 (m, 5H, arom), 7.92−7.98 (m, 4H, arom), 12.10 (s, 1H, NH) ppm: ¹³C NMR (CDCl₃) δ 20.01, 117.30, 125.77, 127.18, 128.85, 130.36, 131.47, 131.53, 131.63, 131.79, 132.07, 132.16, 134.23, 134.41, 139.42, 145.81 ppm. Anal. (C₂₁H₁₅BrClN₃O₂S₂) C, H, N.

4-Chloro-2-mercapto-5-methyl-N-[3-(3-nitrobenzoyl)-quinoxalin-2-yl]benzene-sulfonamide (62). Starting from

6-chloro-7-methyl-3-(3-nitrobenzoyl)-1,1-dioxo-1,4,2-benzodithiazine (1.59 g), the compound **62** was obtained (1.7 g, 87%): mp 211−212 °C dec: IR (KBr) 3220, 3155 (NH), 2525 (SH), 1610 (C=N), 1350, 1130 (SO₂) cm⁻¹; ¹H NMR (DMSO-d_6) δ 2.30 (s, 1H, SH), 2.33 (s, 3H, CH₃), 7.55−7.63 (m, 1H, arom), 7.71−7.79 (m, 3H, arom.), 7.96−8.06 (m, 3H, arom), 8.30−8.36 (m, 2H, arom), 8.72 (t, J = 1.9 Hz, 1H, H-2, PhNO₂), 11.70 (br.s, 1H, NH) ppm; ¹³C NMR (DMSO-d_6) δ 19.12, 124.68, 124.83, 127.02, 129.28, 129.73, 130.85, 131.34, 131.92, 132.43, 133.03, 136.21, 136.44, 137.02, 137.36, 137.54, 144.53, 147.46 ppm. Anal. (C₂₁H₁₅ClN₄O₄S₂) C, H, N.

General Procedure for the Preparation of 5-Carbamoyl-4-chloro-2-mercapto-N-(4H-1,2,4-triazol-3-yl)benzenesulfonamides 63−66, 75, and 77. To a stirred solution of appropriate **B-1**−**B-6** (5 mmol) in dry DMF (4.6 mL) was added 99% hydrazine hydrate (2.25 g, 45 mmol) under dry nitrogen and the solution was heated at 100 °C for 15 h. After the sample was cooled to room temperature, the reaction mixture was diluted with cold water (75 mL) and acidified to pH 2.5 with 2% hydrochloric acid, and then stirred at room temperature for 0.5 h. The resulting precipitate was separated by suction, washed with cold water, and dried. The crude product thus obtained was suspended in water (20 mL) and treated with 5% aqueous NaOH (1 molar equiv). The suspension was stirred at room temperature for 20 min, and the insoluble material was filtered off. The filtrate was immediately acidified to pH 3.0 with 2% hydrochloric acid, and the solid product that deposited was collected by filtration, washed with water (3 × 1.5 mL), and dried at temperatures gradually increased to 90 °C.

In this manner, the following benzenesulfonamides were obtained:

4-Chloro-N-[4-(4-chlorophenyl)-4H-1,2,4-triazol-3-yl]-2-mercapto-5-phenyl-carbamoylbenzenesulfonamide (63). Starting from **B-1** (2.39 g, 5 mmol) the compound **63** was obtained (1.6 g, 61%): mp 145−147 °C dec; IR (KBr) 3295, 3195 (NH), 2549 (SH), 1654 (C=O), 1313, 1140 (SO₂) cm⁻¹; ¹H NMR (DMSO-d_6) δ 7.05−7.52 (m, 5H), 7.67−7.78 (m, 5H), 7.82 (s, 1H), 8.22 (s, 1H), 8.70 (s, 1H), 10.57 (s, 1H) ppm; ¹³C NMR (DMSO-d_6) δ 119.53, 123.99, 126.78, 128.38, 128.74, 129.17, 130.92, 131.27, 132.17, 133.42, 134.34, 137.23, 137.52, 138.66, 139.16, 148.22, 162.80 ppm. Anal. (C₂₁H₁₅Cl₂N₅O₃S₂) C, H, N.

4-Chloro-2-mercapto-N-[4-(4-methylphenyl)-4H-1,2,4-triazol-3-yl]-5-phenyl-carbamoylbenzenesulfonamide (64). Starting from **B-2** (2.29 g, 5 mmol) the compound **64** was obtained (1.4 g, 56%): mp 136−138 °C dec; IR (KBr) 3454, 3289 (NH), 2554 (SH), 1663 (C=O), 1340, 1140 (SO₂) cm⁻¹; ¹H NMR (DMSO-d_6) δ 2.32 (s, 3H), 7.12−7.50 (m, 8H), 7.58−7.80 (m, 3H), 8.22 (s, 1H), 8.65 (s, 1H), 10.57 (s, 1H) ppm; ¹³C NMR (DMSO-d_6) δ 20.52, 119.57, 123.96, 124.85, 128.78, 129.10, 129.63, 129.88, 130.85, 132.17, 132.88, 136.84, 137.26, 137.66, 138.80, 139.40, 148.33, 163.03 ppm. Anal. (C₂₂H₁₈ClN₅O₃S₂) C, H, N.

4-Chloro-5-(4-fluorophenylcarbamoyl)-N-[4-(4-fluorophenyl)-4H-1,2,4-triazol-3-yl]-2-mercaptobenzenesulfonamide (65). Starting from **B-3** (2.4 g, 5 mmol) the title compound **65** was obtained (1.8 g, 69%): mp 137−141 °C dec; IR (KBr) 3248, 3142 (NH), 2554 (SH), 1648 (C=O), 1354, 1143 (SO₂) cm⁻¹; ¹H NMR (DMSO-d_6) δ 7.13−7.49 (m, 5H), 7.60−7.88 (m, 5H), 8.22 (s, 1H), 8.67 (s, 1H), 10.62 (s, 1H) ppm; ¹³C NMR (DMSO-d_6) δ 113.94, 114.43, 115.81, 120.60, 126.26, 126.76, 128.19, 129.72, 130.76, 131.80, 133.92, 136.14, 136.58, 138.11, 143.0, 147.23, 162.38 ppm. Anal. (C₂₁H₁₄ClF₂N₅O₃S₂) C, H, N.

4-Chloro-5-(4-chlorophenylcarbamoyl)-N-[4-(4-fluorophenyl)-4H-1,2,4-triazol-3-yl]-2-mercaptobenzenesulfonamide (66). Starting from **B-4** (2.48 g, 5 mmol) the compound **66** was obtained (1.7 g, 63%): mp 197−199 °C dec; IR (KBr) 3283 (NH), 2543 (SH), 1663 (C=O), 1346, 1307, 1140 (SO₂) cm⁻¹; ¹H NMR (DMSO-d_6) δ 7.25−7.50 (m, 4H), 7.58−7.83 (m, 6H), 8.20 (s, 1H), 8.65 (s, 1H), 10.67 (s, 1H) ppm; ¹³C NMR (DMSO-d_6) δ 114.88, 115.86, 121.07, 125.78, 126.37,

127.75, 129.82, 130.71, 132.92, 133.18, 135.18, 136.63, 138.11, 138.36, 146.98, 147.48, 162.28 ppm. Anal. ($C_{21}H_{14}Cl_2FN_5O_3S_2$) C, H, N.

4-Chloro-N-[4-(4-fluorophenyl)-4H-1,2,4-triazol-3-yl]-2-mercapto-5-phenyl-carbamoylbenzenesulfonamide (75). Starting from **B-5** (2.3 g, 5 mmol) the compound **75** was obtained (1.5 g, 59%): mp 220−223 °C dec; IR (KBr) 3283, 3148 (NH), 2543 (SH), 1683 (C=O), 1346, 1140 (SO$_2$) cm^{-1}; ^{1}H NMR (DMSO-d_6) δ 7.13−7.50 (m, 6H), 7.60−7.83 (m, 5H), 8.20 (s, 1H), 8.68 (s, 1H), 10.55 (s, 1H) ppm; ^{13}C NMR (DMSO-d_6) δ 115.47, 116.64, 119.53, 124.10, 127.74, 128.71, 128.95, 130.85, 132.88, 134.20, 134.45, 137.19, 138.66, 139.34, 139.69, 148.36, 162.99 ppm. Anal. ($C_{21}H_{15}ClFN_5O_3S_2$) C, H, N.

4-Chloro-5-(4-chlorophenylcarbamoyl)-2-mercapto-N-[4-(4-methylphenyl)-4H-1,2,4-triazol-3-yl]benzenesulfonamide (76). Starting from **B-6** (2.46 g, 5 mmol) the compound **76** was obtained (1.9 g, 71%): mp 138−140 °C dec; IR (KBr) 3301, 3189 (NH), 2537 (SH), 1672 (C=O), 1340, 1143 (SO$_2$) cm^{-1}; ^{1}H NMR (DMSO-d_6) δ 2,32 (s, 3H), 7.25−7.57 (m, 6H), 7.68−7.83 (m, 4H), 8.22 (s, 1H), 8.64 (s, 1H), 10.72 (s, 1H) ppm; ^{13}C NMR (DMSO-d_6) δ 20.52, 120.30, 121.07, 124.25, 126.76, 127.85, 128.24, 128.74, 129.13, 130.12, 130.83, 131.77, 136.50, 136.65, 137.62, 138.55, 147.43, 162.38 ppm. Anal. ($C_{22}H_{17}Cl_2N_5O_3S_2$) C, H, N.

General Procedure for the Preparation of 5-Carbamoyl-4-chloro-2-mercapto-N-(4H-1,2,4-triazol-3-yl)benzenesulfonamides 67−74. To a stirred solution of appropriate **B-7**−**B-14** (5 mmol) in dry DMF (4.6 mL) was added 99% hydrazine hydrate (2.25 g, 45 mmol) under dry nitrogen and the solution was heated at 100 °C for 10−11 h. After the sample was cooled to room temperature, the reaction mixture was diluted with cold water (75 mL), acidified to pH 2.5 with 2% hydrochloric acid, and then stirred for 0.5 h at room temperature. The resulting precipitate was filtered off, washed with cold water, and dried. The crude reaction product thus obtained was suspended in water (20 mL), treated with 5% NaOH (1 molar equiv), and stirred vigorously for 20 min at room temperature. The insoluble side product was filtered off, and the filtrate was immediately acidified with 2% hydrochloric acid to pH 3.0. The pure product thus obtained was collected by filtration, washed with water (3 × 1.5 mL), and dried at temperature gradually increasing to 80 °C.

In this manner, the following benzenesulfonamides were obtained:

4-Chloro-2-mercapto-5-(4-methylphenylcarbamoyl)-N-(4-propyl-4H-1,2,4-triazol-3-yl)benzenesulfonamide (67). Starting from **B-7** (2.12 g, 5 mmol) the compound **67** was obtained (1.7 g, 72%): mp 122−124 °C dec; IR (KBr) 3277, 3227, 3142 (NH), 2543 (SH), 1654 (C=O), 1313, 1140 (SO$_2$) cm^{-1}; ^{1}H NMR (CDCl$_3$) δ 0.85 (t, J = 7.5 Hz, 3H), 1.45−1.80 (m, 2H), 2.30 (s, 3H), 3.50−3.75 (t, J = 7.5 Hz, 2H), 6.50 (b.s, 1H), 7.07 (d, J = 8.5 Hz, 2H), 7.45 (d, J = 8.5 Hz, 2H), 7.65 (s, 1H), 8.28 (s, 1H), 8.68 (s, 1H) ppm; ^{13}C NMR (CDCl$_3$) δ 10.84, 20.91, 22.05, 45.63, 120.35, 129.42, 129.78, 131.77, 131.88, 134.45, 134.70, 135.08, 136.84, 137.59, 138.88, 149.40, 163.42 ppm. Anal. ($C_{19}H_{20}ClN_5O_3S_2$) C, H, N.

N-(4-Butyl-4H-1,2,4-triazol-3-yl)-4-chloro-5-(4-chlorophenylcarbamoyl)-2-mercaptobenzenesulfonamide (68). Starting from **B-8** (2.29 g, 5 mmol) the title compound **68** was obtained (1.5 g, 60%): mp 129−132 °C dec; IR (KBr) 3406, 307, 3160 (NH), 2549 (SH), 1657 (C=O), 1310, 1143 (SO$_2$) cm^{-1}; ^{1}H NMR (CDCl$_3$) δ 0.87 (t, J = 7.5 Hz, 3H), 1.05−1.45 (m, 2H), 1.50−1.78 (m, 2H), 3.70 (t, J = 7.5 Hz, 2H), 7.20−7.30 (m, 3H), 7.55−7.68 (m, 3H), 8.27 (s, 1H), 8.90 (s, 1H) ppm; ^{13}C NMR (CDCl$_3$) δ 13.41, 19.66, 30.68, 44.10, 121.64, 128.88, 129.70, 131.49, 131.95, 134.77, 136.40, 137.02, 137.50, 138.51, 138.94, 149.43, 163.74 ppm. Anal. ($C_{19}H_{19}Cl_2N_5O_3S_2$) C, H, N.

N-(4-Butyl-4H-1,2,4-triazol-3-yl)-4-chloro-2-mercapto-5-(4-methylphenylcarbamoyl)benzenesulfonamide (69). Starting from **B-9** (2.19 g, 5 mmol) the compound **69** was obtained (1.3 g, 55%): mp 107−110 °C dec; IR (KBr) 3277, 3248, 3195 (NH), 2543 (SH), 1648 (C=O), 1313, 1140 (SO$_2$) cm^{-1}; ^{1}H NMR (CDCl$_3$) δ 0.88 (t, J = 7.5 Hz, 3H), 1.05−1.40 (m, 2H), 1.48−1.75 (m, 2H), 2.30 (s, 3H), 3.72 (t, J = 7.5 Hz, 2H), 6.63 (b.s, 1H), 7.08 (d, J = 8.5 Hz, 2H), 7.50 (d, J = 8.5

Hz, 2H), 7.65 (s, 1H), 8.30 (s, 1H), 8.65 (s, 1H) ppm; ^{13}C NMR (CDCl$_3$) δ 13.42, 19.59, 20.91, 30.62, 43.89, 120.36, 129.42, 129.74, 131.60, 131.62, 134.45, 135.06, 135.55, 136.88, 137.63, 138.45, 149.40, 163.42 ppm. Anal. ($C_{20}H_{22}ClN_5O_3S_2$) C, H, N.

N-(4-Butyl-4H-1,2,4-triazol-3-yl)-4-chloro-2-mercapto-5-(phenylmethyl-carbamoyl)benzenesulfonamide (70). Starting from **B-10** (2.19 g, 5 mmol) the compound **70** was obtained (1.2 g, 50%): mp 103−105 °C dec; IR (KBr) 3325, 3148 (NH), 2549 (SH), 1655 (C=O), 1331, 1140 (SO$_2$) cm^{-1}; ^{1}H NMR (CDCl$_3$) δ 0.87 (t, J = 7.5 Hz, 3H), 1.08−1.75 (m, 4H), 3.45 (s, 1H), 3.72 (t, J = 7.5 Hz, 2H), 4.55 (d, J = 8 Hz, 2H), 6.90 (t, J = 8 Hz, 1H), 7.27 (s, 5H), 7.35 (s, 1H), 7.57 (s, 1H), 8.35 (s, 1H) ppm; ^{13}C NMR (DMSO-d_6) δ 13.45, 19.62, 30.95, 44.06, 44.10, 127.46, 127.78, 128.59, 130.09, 131.06, 131.84, 134.24, 137.30, 137.73, 138.05, 138.55, 149.54, 165.21 ppm. Anal. ($C_{20}H_{22}ClN_5O_3S_2$) C, H, N.

4-Chloro-5-(4-chlorophenylcarbamoyl)-2-mercapto-N-[4-(2-methylpropyl)-4H-1,2,4-triazol-3-yl]benzenesulfonamide (71). Starting from **B-11** (2.29 g, 5 mmol) the compound **71** was obtained (1.8 g, 72%): mp 130−132 °C dec; IR (KBr) 3372, 3301, 3154 (NH), 2555 (SH), 1663 (C=O), 1307, 1149 (SO$_2$) cm^{-1}; ^{1}H NMR (CDCl$_3$) δ 0.85 (d, J = 7.5 Hz, 6H), 1.85−2.20 (m, 1H), 3.55 (d, J = 7.5 Hz, 2H), 7.20−7.32 (m, 3H), 7.55−7.70 (m, 3H), 8.25 (s, 1H), 8.98 (s, 1H) ppm; ^{13}C NMR (CDCl$_3$) δ 19.66, 27.94, 51.20, 121.64, 128.85, 129.81, 131.42, 131.85, 134.74, 136.45, 137.02, 137.48, 138.91, 139.20, 148.58, 163.49 ppm. Anal. ($C_{19}H_{19}Cl_2N_5O_3S_2$) C, H, N.

4-Chloro-2-mercapto-5-(4-methoxyphenylcarbamoyl)-N-[4-(2-methylpropyl)-4H-1,2,4-triazol-3-yl]benzenesulfonamide (72). Starting from **B-12** (2.27 g, 5 mmol) the compound **72** was obtained (1.5 g, 61%): mp 138−140 °C dec; IR (KBr) 3365, 3265, 3148 (NH), 2560 (SH), 1681 (C=O), 1299, 1138 (SO$_2$) cm^{-1}; ^{1}H NMR (DMSO-d_6) δ 0.82 (d, J = 7.5 Hz, 6H), 1.88−2.25 (m, 1H), 3.62 (d, J = 7.5 Hz, 2H), 3.75 (s, 3H), 6.95 (d, J = 11 Hz, 2H), 7.62 (d, J = 11 Hz, 2H), 7.80 (s, 1H), 8.20 (s, 1H), 8.40 (s, 1H) ppm; ^{13}C NMR (DMSO-d_6) δ 19.23, 27.18, 49.74, 55.13, 113.86, 121.07, 128.76, 130.50, 131.74, 132.16, 132.74, 136.98, 137.77, 139.98, 148.65, 155.64, 163.64 ppm. Anal. ($C_{20}H_{22}ClN_5O_4S_2$) C, H, N.

4-Chloro-2-mercapto-5-(4-methylphenylcarbamoyl)-N-[4-(1-methylpropyl)-4H-1,2,4-triazol-3-yl]benzenesulfonamide (73). Starting from **B-13** (2.19 g, 5 mmol) the compound **73** was obtained (1.9 g, 79%): mp 120−122 °C dec; IR (KBr) 3295, 3195, 3136 (NH), 2543 (SH), 1654 (C=O), 1313, 1137 (SO$_2$) cm^{-1}; ^{1}H NMR (CDCl$_3$) δ 0.80 (t, J = 7 Hz, 3H), 1.32 (d, J = 7 Hz, 3H), 1.50−1.82 (m, 2H), 2.31 (s, 3H), 4.08−4.38 (m, 1H), 7.10 (d, J = 9 Hz, 2H), 7.45−7.70 (m, 4H), 8.32 (s, 1H), 8.68 (s, 1H) ppm; ^{13}C NMR (CDCl$_3$) δ 10.24, 19.59, 20.91, 28.72, 52.70, 120.32, 129.81, 129.42, 131.66, 131.77, 134.45, 135.09, 136.23, 136.80, 137.73, 149.19, 163.35 ppm. Anal. ($C_{20}H_{22}ClN_5O_3S_2$) C, H, N.

N-(4-Benzyl-4H-1,2,4-triazol-3-yl)-4-chloro-2-mercapto-5-(4-methylphenyl-carbamoyl)benzenesulfonamide (74). Starting from **B-14** (2.36 g, 5 mmol) the compound **74** was obtained (1.9 g, 74%): mp 170−172 °C dec; IR (KBr) 3283, 3142 (NH), 2531 (SH), 1663 (C=O), 1313, 1139 (SO$_2$) cm^{-1}; ^{1}H NMR (DMSO-d_6) δ 2.32 (s, 3H), 5.05 (s, 2H), 7.20 (d, J = 8 Hz, 2H), 7.40 (s, 6H), 7.65 (d, J = 8 Hz, 2H), 7.85 (s, 1H), 8.22 (s, 1H), 8.55 (s, 1H), 10.30 (s, 1H) ppm; ^{13}C NMR (DMSO-d_6) δ 20.41, 46.10, 119.57, 127.88, 128.08, 128.63, 129.13, 130.77, 132.24, 132.95, 133.15, 135.19, 137.12, 136.16, 137.73, 139.67, 148.76, 163.28 ppm. Anal. ($C_{23}H_{20}ClN_5O_3S_2$) C, H, N.

Synthesis of N-(4-Butyl-4H-1,2,4-triazol-3-yl)-5-carbamoyl-4-chloro-2-mercapto-benznesulfonamide (C-1). To a stirred solution of **B-15** (2.29 g, 5 mmol) in dry DMF (4.6 mL) 99% hydrazine hydrate (1.5 g, 30 mmol) was added under dry nitrogen and the reaction mixture was heated at 100 °C for 4 h. After the sample was cooled to room temperature, the solution was diluted with cold water (75 mL), acidified to pH 2.5 with 2% hydrochloric acid, and then stirred for 0.5 h at room temperature. The solid that precipitated was collected by filtration, washed with cold water, and dried. The crude product thus obtained was purified by crystallization from glacial acetic acid and dried at 100 °C to afford **C-1** (1.7 g, 89%): mp 224−225 °C dec; IR (KBr) 3477, 3454, 3312, 3148

(NH$_2$, NH), 2537 (SH), 1666 (C=O), 1316, 1143 (SO$_2$) cm^{-1}; ^{1}H NMR (DMSO-d_6) δ 0.85 (t, $J = 7.5$ Hz, 3H), 1.05−1.37 (m, 2H), 1.45−1.85 (m, 2H), 3.77 (t, $J = 7.5$ Hz, 3H), 7.72 (s, 1H), 7.95 (b.s, 2H), 8.12 (s, 1H), 8.84 (s, 1H), 13.15 (b.s, 1H) ppm; ^{13}C NMR (DMSO-d_6) δ 13.27, 18.94, 30.00, 42.81, 128.77, 132.16, 130.77, 134.73, 136.48, 137.83, 139.87, 148.65, 166.70 ppm. Anal. (C$_{13}$H$_{16}$ClN$_5$O$_3$S$_2$) C, H, N.

General Procedure for the Preparation of 4-Carbamoyl-5-chloro-2-[(4H-1,2,4-triazol-3-yl)aminosulfonyl]phenylthioacetic Acids 77, 78. A vigorously stirred suspension of appropriate compound **C-1** or **67** (5 mmol) and NaOH (0.2 g, 5 mmol) in water (10 mL) was treated dropwise with a solution of chloroacetic acid (0.47 g, 5 mmol) and Na$_2$CO$_3$ (0.26 g, 2.5 mmol) in water (12 mL). The reaction mixture was heated at 40 °C for 1 h, and then the temperature was raised to 90 °C at the rate of 10 °C/h. The solution was further stirred at 90 °C for 20 h, and then was left to stand overnight at ambient temperature. The reaction mixture (pH 6.6) was neutralized to pH 7.2−7.8 with aqueous 10% Na$_2$CO$_3$. The side-product that precipitated was filtered off, and the filtrate was acidified to pH 2.5 with 2% hydrochloric acid. The crude product that deposited was collected by filtration, washed with water, dried, and purified by crystallization from 2-propanol.

In this manner, the following acetic acid derivatives were obtained:

2-[(4-Butyl-4H-1,2,4-triazol-3-yl)aminosulfonyl]-4-carbamoyl-5-chlorophenyl-thioacetic acid (77). Starting from **C-1** (1.95 g, 5 mmol) the compound **77** was obtained (1.4 g, 63%): mp 114−116 °C dec; IR (KBr) 3430−2850 (OH), 3412, 3307, 3237 (NH$_2$, NH), 1733 (C=O), 1639 (C=O), 1319, 1137 (SO$_2$) cm^{-1}; ^{1}H NMR (DMSO-d_6) δ 0.83 (t, $J = 7.5$ Hz, 3H), 1.0−1.35 (m, 2H), 1.45−1.72 (m, 2H), 3.82 (t, $J = 7.5$ Hz, 2H), 3.95 (s, 2H), 7.45 (s, 1H), 7.68 (b.s, 1H), 7.99 (b.s, 1H), 8.1 (s, 1H), 8.37 (s, 1H) ppm; ^{13}C NMR (DMSO-d_6) δ 13.27, 18.95, 29.97, 34.15, 42.53, 127.13, 128.71, 131.99, 133.16, 138.16, 139,50, 139.91, 148.72, 166.78, 169.88 ppm. Anal. (C$_{15}$H$_{18}$ClN$_5$O$_5$S$_2$) C, H, N.

5-Chloro-4-(4-methylphenylcarbamoyl)-2-(4-propyl-4H-1,2,4-triazol-3-yl)aminosulfonyl)phenylthioacetic acid (78). Starting from **67** (2.33 g, 5 mmol) the compound **78** was obtained (1.7 g, 66%): mp 232−234 °C dec; IR (KBr) 3315−2830 (OH), 3307, 3184, 3154 (NH), 1710 (C=O), 1669 (C=O), 1310, 1137 (SO$_2$) cm^{-1}; ^{1}H NMR (DMSO-d_6) δ 0.80 (t, $J = 7.5$ Hz, 3H), 1.51−1−85 (m, 2H), 2.28 (s, 3H), 3.70 (t, $J = 7.5$ Hz, 2H), 4.05 (s, 2H), 7.16 (d, $J = 9.5$ Hz, 2H), 7.55 (s, 1H), 7,60 (d, $J = 9.5$ Hz, 2H), 8.20 (s, 1H), 8.38 (s, 1H), 10.53 (s, 1H) ppm; ^{13}C NMR (DMSO-d_6) δ 10.49, 20.41, 21.34, 34.08, 44.60, 119,57, 127.03, 129.09, 131.90, 132.06, 132.95, 133.34, 136.16, 138.23, 139.77, 148.79, 163.35, 169.92 ppm. Anal. (C$_{21}$H$_{22}$ClN$_5$O$_5$S$_2$) C, H, N.

Chemicals. For IN assays, all compounds were dissolved in DMSO, and all aliquots were also made in DMSO prior to each experiment. The stock solutions were kept at −20 °C.

Preparation of Oligonucleotide Substrates. The oligonucleotides 21top, 5′-GTGTGGAAAATCTCTAGCAGT-3′ and 21bot, 5′-ACTGCTAGAGATTTTCCACAC-3′ were purchased from Norris Cancer Center Core Facility (University of Southern California) and purified by UV shadowing on polyacrylamide gel as described. To analyze the extent of 3′-processing and strand transfer using 5′-end labeled substrates, 21top was 5′-end labeled using T$_4$ polynucleotide kinase (Epicenter, Madison, WI) and γ[^{32}P]-ATP (Amersham Biosciences). The kinase was heat-inactivated and 21bot was added in 1.5-molar excess. The mixture was heated at 95 °C, allowed to cool slowly to room temperature, and run through a spin 25 mini-column (USA Scientific) to separate annealed double-stranded oligonucleotide from unincorporated material.

Integrase Assay. To determine the extent of 3′-processing and strand transfer, HIV-1 IN was preincubated at a final concentration of 200 nM with the inhibitor in reaction buffer (50 mM NaCl, 1 mM HEPES, pH 7.5, 50 μM EDTA, 50 μM dithiothreitol, 10% glycerol (w/v), 7.5 mM MnCl$_2$, 0.1 mg/mL bovine serum albumin, 10 mM 2-mercaptoethanol, 10% DMSO, and 25 mM MOPS, pH 7.2) at 30 °C for 30 min. Then, 20 nM of the 5′-end ^{32}P-labeled linear oligonucleotide substrate was

added, and incubation was continued for an additional 1 h. Reactions were quenched by an addition of (8 μL) of loading dye (98% deionized formamide, 10 mM EDTA, 0.025% xylene cyanol, and 0.025% bromophenol blue). An aliquot (5 μL) was electrophoresed on a denaturing 20% polyacrylamide gel (0.09 M tris-borate pH 8.3, 2 mM EDTA, 20% acrylamide, 8 M urea). Gels were dried, exposed on a PhosphorImager cassette, read on a Typhoon 8610 Variable Mode imager (Amersham Biosciences), and quantitated using ImageQuant 5.2 (Amersham Biosciences).

Molecular Modeling and Alignment. The structures were built in SYBYL 6.7[29] on a Silicon Graphics Octane (R12000) workstation. Two different conformational templates were used in the QSAR studies. These were derived by (i) FlexX docking of compound **1** or (ii) performing a systematic conformational search in SYBYL. Compound **1** was docked onto the active site of HIV-1 IN using the FlexX docking program interfaced with SYBYL. Among the 30 conformations and binding modes generated, the highest scored conformation by FlexX scoring function was used as a template to build all the molecules in one conformational set, which is referred to as "Conf-d". The other conformational template was obtained by systematic conformational search of compound **14**. In the conformational search, all the rotatable bonds (a−d, Figure 1) in compound **14** were varied by 10°. The lowest energy conformation identified in this conformational search was used as a template to build the molecules in the second conformational set, which is referred to as "Conf-s". The molecules in each conformational set constructed using the respective templates were superimposed using the multifit function in SYBYL and energy minimized using the Powell conjugate gradient methods.[29] The common structure highlighted in compound **1** (Figure 1) that includes the six aromatic carbon, sulfur, two oxygen, and nitrogen atoms were used for aligning the molecules. Charges were calculated using the semiemperical method AM1 in MOPAC 6.0,[30] interfaced with SYBYL.

CoMFA and CoMSIA Studies. The CoMFA descriptors, steric (Lennard-Jones 6−12 potential) and electrostatic (Coulombic potential) field energies, were calculated using the SYBYL default parameters: 2 Å grid points spacing, an sp3 carbon probe atom with +1 charge and a van der Waals radius of 1.52 Å, and energy cutoff of 30 kcal/mol.

The five similarity indices in CoMSIA, i.e., steric, electrostatic, hydrophobic, H-bond donor, and H-bond acceptor descriptors, were calculated[31] using a C^{1+} probe atom with a radius of 1.0 Å placed at regular grid spacing of 2 Å. CoMSIA similarity indices (A_F) for a molecule j with atoms i at a grid point q are calculated by eq 1:

$$A_{F,k}{}^q(j) = -\Sigma\omega_{\text{probe},k}\omega_{ik}e^{-\alpha r_{iq}^2} \tag{1}$$

where k represents the following physicochemical properties: steric, electrostatic, hydrophobic, H-bond donor, and H-bond acceptor. A Gaussian type distance dependence was used between the grid point q and each atom i of the molecule. The default value of 0.3 was used as the attenuation factor (α). Here, steric indices are related to the third power of the atomic radii, electrostatic descriptors are derived from atomic partial charges, hydrophobic fields are derived from atom-based parameters,[32] and H-bond donor and acceptor indices are obtained by a rule-based method based on experimental results.[33]

The CoMFA and CoMSIA descriptors derived above were used as explanatory variables, and pIC$_{50}$ ($-\log$ IC$_{50}$) values were used as the target variable in PLS regression analyses to derive 3D QSAR models using the implementation in the SYBYL package. The predictive value of the models was evaluated by leave-one-out (LOO) cross-validation. The cross-validated coefficient, q^2, was calculated using eq 2:

$$q^2 = 1 - \frac{\sum(Y_{\text{predicted}} - Y_{\text{observed}})^2}{\sum(Y_{\text{observed}} - Y_{\text{mean}})^2} \tag{2}$$

where Y_{pred}, Y_{actual}, and Y_{mean} are predicted, actual, and mean

values of the target property (pIC_{50}), respectively. $\Sigma(Y_{pred} - Y_{actual})^2$ is the predictive sum of squares (PRESS). To maintain the optimum number of PLS components and minimize over determination, the number of components giving the lowest PRESS value was used for deriving the final PLS regression models. Conventional correlation coefficient r^2 and its standard error, s, were also computed for the final PLS models. CoMFA and CoMSIA coefficient maps were generated by interpolation of the pairwise products between the PLS coefficients and the standard deviations of the corresponding CoMFA or CoMSIA descriptor values.

FlexX Docking. The FlexX program[34] version 1.9 interfaced with SYBYL 6.7 was used to dock the compounds onto the active site of HIV-1 IN. FlexX is a fast automated docking program that considers ligand conformational flexibility by an incremental fragment placing technique.[34,35] We used the program to dock the training set as well as the test set molecules into the active site of monomeric unit "A" of the crystal structure of the HIV-1 IN catalytic core. The 3D coordinates of the HIV-1 IN catalytic core in complex with an inhibitor were taken from the Brookhaven Protein Databank (PDB code: 1QS4).[9] The missing residues at positions 141–144 were inserted by means of the loop search algorithm in the SYBYL BIOPOLYMER module. The active site for docking was defined as all atoms within 6.5 Å radius of the cocrystallized ligand. The default SYBYL FlexX parameters were used.

References

(1) Brown, P. O. *Integration*; Cold Spring Harbor Press: Cold Spring Harbor, NY, 1999.
(2) Asante-Appiah, E.; Skalka, A. M. HIV-1 integrase: structural organization, conformational changes, and catalysis. *Adv. Virus Res.* **1999**, *52*, 351–369.
(3) Neamati, N. Patented small molecule inhibitors of HIV-1 integrase: a ten-year saga. *Expert Opin. Ther. Pat.* **2002**, *12*, 709–724.
(4) Dayam, R.; Neamati, N. Small-Molecule HIV-1 Integrase Inhibitors: the 2001–2002 Update. *Curr. Pharm. Des.* **2003**, *9*, 1789–1802.
(5) Neamati, N.; Barchi, J. J., Jr. New paradigms in drug design and discovery. *Curr. Top. Med. Chem.* **2002**, *2*, 211–227.
(6) Neamati, N.; Mazumder, A.; Sunder, S.; Owen, J. M.; Schultz, R. J.; Pommier, Y. 2-Mercaptobenzenesulfonamides as novel class of human immunodeficiency type 1 (HIV-1) integrase and HIV-1 replication. *Antimicrob. Agents Chemother.* **1997**, *8*, 485–495.
(7) Nicklaus, M. C.; Neamati, N.; Hong, H.; Mazumder, A.; Sunder, S.; Chen, J.; Milne, G. W.; Pommier, Y. HIV-1 integrase pharmacophore: discovery of inhibitors through three- dimensional database searching. *J. Med. Chem.* **1997**, *40*, 920–929.
(8) Lubkowski, J.; Yang, F.; Alexandratos, J.; Wlodawer, A.; Zhao, H.; Burke, T. R., Jr.; Neamati, N.; Pommier, Y.; Merkel, G.; Skalka, A. M. Structure of the catalytic domain of avian sarcoma virus integrase with a bound HIV-1 integrase-targeted inhibitor. *Proc. Natl. Acad. Sci. U.S.A.* **1998**, *95*, 4831–4836.
(9) Neamati, N.; Mazumder, A.; Zhao, H.; Sunder, S.; Burke, T. R., Jr.; Schultz, R. J.; Pommier, Y. Diarylsulfones, a novel class of human immunodeficiency virus type 1 integrase inhibitors. *Antimicrob. Agents Chemother.* **1997**, *41*, 385–393.
(10) Chen, I. J.; Neamati, N.; Nicklaus, M. C.; Orr, A.; Anderson, L.; Barchi, J. J., Jr.; Kelley, J. A.; Pommier, Y.; MacKerell, A. D., Jr. Identification of HIV-1 integrase inhibitors via three-dimensional database searching using ASV and HIV-1 integrases as targets. *Bioorg. Med. Chem.* **2000**, *8*, 2385–2398.
(11) Neamati, N.; Lin, Z.; Karki, R. G.; Orr, A.; Cowansage, K.; Strumberg, D.; Pais, G. C.; Voigt, J. H.; Nicklaus, M. C.; Winslow, H. E.; Zhao, H.; Turpin, J. A.; Yi, J.; Skalka, A. M.; Burke, T. R., Jr.; Pommier, Y. Metal-dependent inhibition of HIV-1 integrase. *J. Med. Chem.* **2002**, *45*, 5661–5670.
(12) Pannecouque, C.; Pluymers, W.; Van Maele, B.; Tetz, V.; Cherepanov, P.; De Clercq, E.; Witvrouw, M.; Debyser, Z. New class of HIV integrase inhibitors that block viral replication in cell culture. *Curr. Biol.* **2002**, *12*, 1169–1177.
(13) Scozzafava, A.; Owa, T.; Mastrolorenzo, A.; Supuran, C. T. Anticancer and antiviral sulfonamides. *Curr. Med. Chem.* **2003**, *10*, 925–953.
(14) Brzozowski, Z. 2-Mercapto-*N*-(azolyl)benzenesulphonamides. I. Synthesis of *N*-(1,1-dioxo-1,4,2-benzodithiazin-3-yl)guanidines and their transformations into 2-mercapto-*N*-(5-amino-1,2,4-triazol-3-yl) benzenesulphonamide derivatives with potential anti-HIV or anticancer activity. *Acta Pol. Pharm.* **1995**, *52*, 91–101.
(15) Brzozowski, Z. 2-Mercapto-*N*-(azolyl)benzenesulphonamides. II. Syntheses, anti-HIV-1 and anticancer activity of some S-substituted 4-chloro-2-mercapto-5-methyl-*N*-(5-amino-1,2,4-triazol-3-yl) benzenesulphonamides. *Acta Pol Pharm.* **1995**, *52*, 287–292.
(16) Brzozowski, Z. 2-mercapto *N*-(azolyl)benzenesulfonamides. VI. Synthesis and anti-HIV activity of some new 2-mercapto-*N*-(1,2,4-triazol-3-yl)benzenesulfonamide derivatives containing the 1,2,4-triazole moiety fused with a variety of heteroaromatic rings. *Acta Pol. Pharm.* **1998**, *55*, 473–480.
(17) Hazuda, D. J.; Felock, P.; Witmer, M.; Wolfe, A.; Stillmock, K.; Grobler, J. A.; Espeseth, A.; Gabryelski, L.; Schleif, W.; Blau, C.; Miller, M. D. Inhibitors of strand transfer that prevent integration and inhibit HI-1 replication in cells. *Science.* **2000**, *287*, 646–650.
(18) Pais, G. C. G.; Burke, T. R. Novel aryl diketo-containing inhibitors of HIV-1 integrase. *Drugs Future* **2002**, *27*, 1101–1111.
(19) Wold, S.; Rhue, A.; Wold, H.; Dunn, W. J. I. The covariance problem in linear regression. The partial least squares (PLS) approach to generalized inverses. *SAIM J. Sci. Stat. Comput.* **1994**, *5*, 735–743.
(20) Wold, S.; Albano, C.; Dunn, W. J., III; Edlund, U.; Esbensen, K.; Geladi, P.; Hellberg, S.; Johanson, E.; Lindberg, W.; Sjostrom, M. Multivariate data analysis in chemistry. *NATO ASI Ser., Ser. C* **1984**, *138*, 17–95.
(21) Clark, M.; Cramer, I., R. D. The probability of chance correlation using partial least squares (PLS). *Quant. Struct-Act Relat.* **1993**, *12*, 137–145.
(22) Brzozowski, Z.; Saczewski, F.; Kuo, C.-L.; Sanchez, T.; Gdaniec, M.; Neamati, N., 2003, unpublished data.
(23) Brzozowski, Z.; Slawinski, J.; Angielski, S.; Szczepanska-Konkiel, M. [Derivatives of 1,1-dioxo-1,4,2-benzodithiazine. III. Synthesis and diuretic properties of 3-(R,R1-phenyl)amino-6-chloro-7-methyl-1,1-dioxo-1,4,2-benzodithiazines]. *Acta Pol. Pharm.* **1985**, *42*, 313–318.
(24) Brzozowski, Z. Syntheses of some new 4-chloro-2-mercapto-*N*-(4H-1,2,4-triazol-3-yl)benzenesulfonamides with potential anticancer or anti-HIV activity. *Acta Pol. Pharm.* **1997**, *54*, 461–466.
(25) Slawinski, J. Synthesis, anti-HIV and anticancer activity of some S-substituted 4-chloro-2-mercapto-5-methyl-*N*-(5-amino-1,2,4-triazol-3-yl)benzenesulfonamides. *Acta Pol. Pharm.* **1995**, *52*, 287–292.
(26) Brzozowski, Z. Synthesis of *N*-(1,1-dioxo-1,4,2-benzodithiazin-3-yl)guanidines and their transformation into 2-mercapto-*N*-(5-amino-1,2,4-triazol-3-yl)benzenesulfonamide derivatives with potential anti-HIV or anticancer activity. *Acta Pol. Pharm.* **1998**, *55*, 91–101.
(27) Brzozowski, Z. Synthesis and anti-HIV activity of some new 2-mercato-*N*-(1,2,4-triazol-3-yl)benzenesulfonamide derivatives containing the 1,2,4-triazole moiety fused with a variety of heteroaromatic rings. *Acta Pol. Pharm.* **1998**, *55*, 473–480.
(28) Brzozowski, Z.; Saczewski, F.; Gdaniec, M. Synthesis, structural characterization and in vitro anticancer activity of 4- dimethyl-aminopyridinium (6-chloro-1,1-dioxo-1,4,2-benzodithiazin-3-yl)-methanides. *Bioorg Med Chem.* **2003**, in press.
(29) *SYBYL Version 6.7*; Tripos Associates: St. Louis, MO.
(30) Stewart, J. J. MOPAC: a semiempirical molecular orbital program. *J. Comput.-Aided Mol. Des.* **1990**, *4*, 1–105.
(31) Klebe, G.; Abraham, U.; Mietzner, T. Molecular similarity indices in a comparative analysis (CoMSIA) of drug molecules to correlate and predict their biological activity. *J. Med. Chem.* **1994**, *37*, 4130–4146.
(32) Viswanadhan, V. N.; Ghose, A. K.; Revenkar, G. R.; Robins, R. Atomic and physichochemical parameters for three-dimensional structure-directed quantitative structure–activity relationships. 4. additional parameters for hydrophobic and dispersive interactions and their application for an automated superposition of certain naturally occurring antibiotics. *J. Chem. Inf. Comput. Sci.* **1989**, *29*, 163–172.
(33) Klebe, G. The use of composite crystal-field environments in molecular recognition and the de novo design of protein ligands. *J. Mol. Biol.* **1994**, *237*, 212–235.
(34) Kramer, B.; Rarey, M.; Lengauer, T. Evaluation of the FLEXX incremental construction algorithm for protein–ligand docking. *Proteins* **1999**, *37*, 228–241.
(35) Rarey, M.; Kramer, B.; Lengauer, T.; Klebe, G. A fast flexible docking method using an incremental construction algorithm. *J. Mol. Biol.* **1996**, *261*, 470–489.